IEEE Access
Multidisciplinary | Rapid Review | Open Access Journal

Received February 4, 2022, accepted February 22, 2022, date of publication February 24, 2022, date of current version March 4, 2022.

Digital Object Identifier 10.1109/ACCESS.2022.3154483

Design of 94GHz Dual-Polarization Antenna Fed by Diagonal Horn for Cloud Radars

JIE WANG[1,2], (Graduate Student Member, IEEE), HAI LIN[1,2], (Graduate Student Member, IEEE), FAN YANG[1], GUANGYANG XU[1], (Student Member, IEEE), AND JUNXIANG GE[1,2,3], (Member, IEEE)

[1]Department of Electronics and Communication, Nanjing University of Information Science and Technology, Nanjing 210044, China
[2]Institute of Electronics Information Technology and System, Nanjing University of Information Science and Technology, Nanjing 210044, China
[3]Jiangsu Key Laboratory of Meteorological Observation and Signal Processing, Nanjing University of Information Science and Technology, Nanjing 210044, China

Corresponding author: Junxiang Ge (jxge@nuist.edu.cn)

This work was supported in part by the National Natural Science Foundation of China under Grant 61671249, and in part by the Jiangsu Innovation and Entrepreneurship Group Talents Plan.

ABSTRACT In this paper, a 94 GHz dual-polarization high-isolation cassegrain antenna feed by a diagonal horn antenna is designed. The antenna consists of a D = 540 mm main reflector, sub-reflector, and dual-port dual-polarization diagonal horn feed antenna. To obtain similar feed horn E-H radiation patterns, gain, high polarization, and port isolation, a dual-port diagonal horn was designed in the feed. The measured antenna gains are 50.85 dBi and the side-lobe levels are −24.5 dB at E-H radiation patterns of two ports at 94 GHz, respectively. The VSWRs of port 1 and port 2 are less than 1.5:1 in the range 93.2–95.3 GHz, which meets the working requirements of frequency modulated continuous wave and pulse cloud radars. And the isolation between the two ports is above −50 dB, whereas the polarization isolation of each port is above 40 dB. The proposed W-band antenna is a suitable candidate for the dual-polarization cloud radars.

INDEX TERMS Cassegrain antenna, diagonal horn antenna, dual-polarization, high isolation, similar beam.

I. INTRODUCTION

Currently, 94 GHz millimeter wave (MMW) weather radars have been developed in recent years because of their excellent ability to investigate the interior structures of clouds and detect the size distributions of cloud particles [1], [2]. Because dual polarization and high isolation characteristics play an important role in the inversion analysis of meteorological targets, the design of dual polarization, high port and polarization isolation, lower side lobes, and high gain antenna becomes significant and important for performance of MMW radars [3]. Generally speaking, as shown in Fig. 1, in order to obtain better detection and identification ability of meteorological particles, considering systematic error, the polarization isolation of weather radar antenna should be better than −30 dB [4].

As a classical antenna, the reflector antenna has an important position in engineering applications owing to its advantages of power, efficiency, and structure [5]–[7].

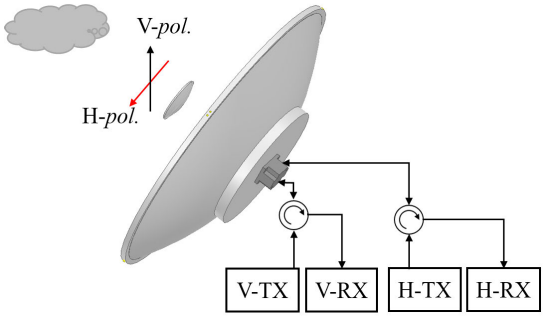

FIGURE 1. Application of W-band dual polarization cassegrain antenna in weather radar.

An innovative way to use a suitable dual polarization transition and receiver system on a existing C-band horn antenna to enable a 100-foot casserain antenna to work in the X-band is introduced in detail in [5]. In [6], a novel high-isolation 35/94-GHz dual-frequency orthogonal cassegrain antenna was designed and analyzed. A three-dimensional (3D) printed cassegrain antenna for THz near-field focusing is used in

The associate editor coordinating the review of this manuscript and approving it for publication was Shah Nawaz Burokur.

back scattered side-channel detection, and the parameters and performance of 3D printed cassegrain antenna were analyzed in [7]. To achieve excellent gain, bandwidth, polarization, and radiation patterns, diagonal horn antennas are widely used in MMW and THz applications [8]–[10]. Two symmetrical pyramidal horn antennas are used to enhance electromagnetic signal collection and radiation in the sub-THz measurement system [8]. A modification of the traditional diagonal horn design using a spline-curve "S" shape modulation in the depth of the "V" groove was introduced in [9]. In [10], the performance of two smooth-walled spline-profile horns, conical and diagonal, was analyzed; the diagonal antenna was found to exhibit very good performance in terms of radiation, cross-polarization level, and efficiency. In [11] and [12], dual-polarization cassegrain antenna is applied in W-band cloud radars. A W-band dual-polarization cassegrain antenna is designed in [13], but the gains is unbalanced, and the difference is 2.2 dB. In [12] and [14], two large aperture antennas are designed and used in space-based W-band MMW cloud radar systems.

In this paper, a 94 GHz dual-polarization high-isolation cassegrain antenna feed using a diagonal horn antenna is designed. The antenna consists of a main reflector, sub-reflector, and diagonal horn feed. The diagonal feed antenna is connected to two orthogonal rectangular waveguide ports. The antenna design and geometry are presented in Section II. The fabrication process and simulated and measured results are discussed in Section III, and the conclusions are provided in Section IV.

II. ANTENNA CONFIGURATION AND DESIGNING

A. DESIGN OF THE CASSEGRAIN ANTENNA CONFIGURATION

Fig. 2 (a) shows the configuration structure of the cassegrain antenna used in the antenna. This antenna includes a rotationally symmetric parabolic main reflector and a rotationally hyperbolic sub-reflector with F_1 as a common focal point [15], [16]. F_2 is the other focus of the hyperbolical reflector, and coincided with the position of the feed horn's phase center. As Fig. 2 (b) shows, the E-Plane of each port of the designed antenna is 45° to the support of the sub-reflector. In this way, the influence of the support structure on the radiation pattern of the two ports is consistent. After considering the mechanical structure, antenna gain, and characteristics of millimeters, the following values are selected:$D = 2R_1 = 540$ mm, $r_1 = 41.5$ mm, $f_1 = 201.8$ mm, $f_2 = 66.8$ mm, $c_1 = 24.8$ mm, $\varphi_0 = 20°$ and $\varphi_1 = 45°$. The value of $\varphi_0 = 20°$ is closely related to -11 dB widths of the E-H plane of the feed horn's radiation patterns. The aforementioned parameters present the design requirements and limits of the antenna feed system.

B. DESIGN OF THE ANTENNA FEED SYSTEM

In comparison with the cone horn and conical horn antenna, the diagonal horn antenna needs to be divided in the matching

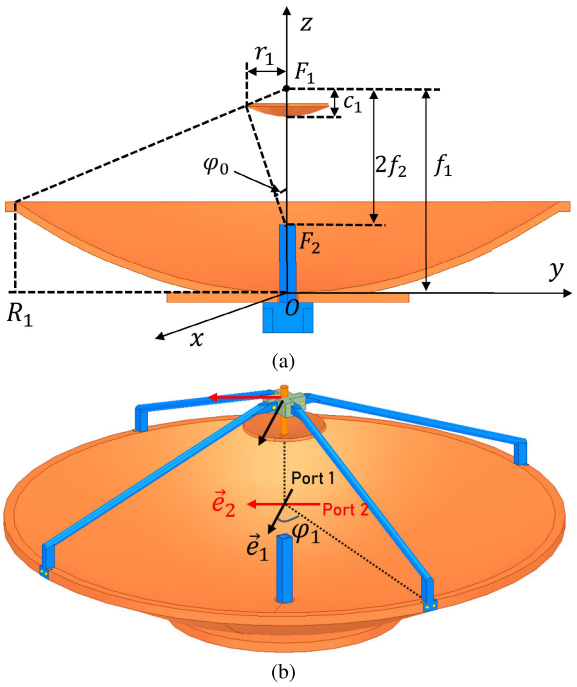

FIGURE 2. (a) side view and (b) the basic three-dimensional geometry of the designed cassegrain antenna.

process; the processing of its internal inclined plane is more complicated. Therefore, they are not commonly used at low frequencies. However, owing to the excellent performance of gain, bandwidth, polarization, and equal E-H radiation patterns, the diagonal horn antenna is a good candidate to replace the corrugated horn in MMW and THz applications.

Therefore, the diagonal horn is selected as the basis of the feed source antenna, and the design and optimization between the antenna and the dual polarization port are realized. Port 1 is located at the straight end of the bottom of the diagonal horn, as shown in Fig. 3 (a), whereas port 2 is located on the side of the diagonal horn and connected by a short reduced height waveguide. Under the condition of bandwidth required for radar applications, the feed method of port 2 is a typical narrow-band method, and good port matching is achieved through a narrow waveguide E-plane step structure [17], [18]. On the other hand, for the compact feed structure, the traditional adjust matching method of screws is hard to apply, and the step structure is benefit to the integration of the antenna feed system. The connection method used in port 2 to the diagonal horn has three advantages. Firstly, it reduces the influence of the opening of port 2 on the current of port 1 and the influence of port 2 on the radiation pattern of the diagonal horn. Secondly, it is conducive for the matching adjustment of port 2. Thirdly, it is conducive for improving the isolation between port 1 and port 2 [19]. Even orthomode transducer (OMT) is widely used in the design of dual-polarization antennas, the traditional OTM methods is hard have an ideal performance in bandwidth, isolation, same beam-form and simple structure [16], [17], [20]. The simple feed method, in out design, is suitable for the design of large

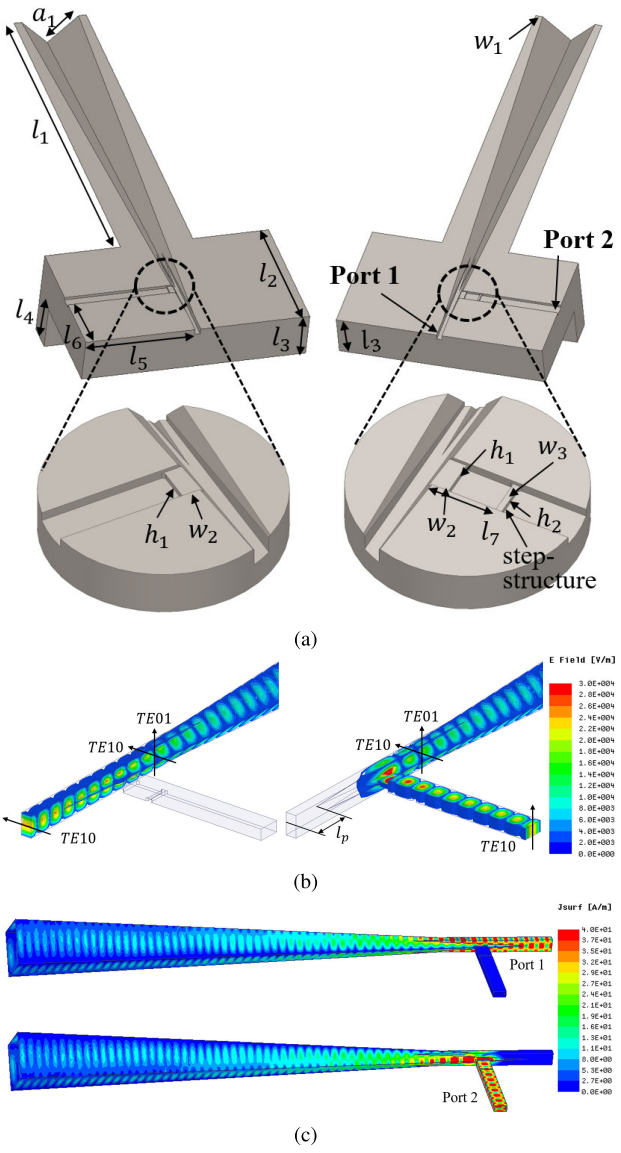

FIGURE 3. (a) Exploded view of the dual-polarization antenna feed horn. (b) Modes of the feed structure and (c) current distributions when two ports are fed respectively.

aperture, small feed size high frequency, high isolation and dual-polarization antennas.

Fig. 3 (b) shows modes of the feed structure, TE10 is the fundamental mode of standard waveguide and we view the diagonal horn antenna as the common port. Modes TE10 and TE01 of common port are two orthogonal modes and correspond to dual-polarization $\vec{e}_1$ and $\vec{e}_2$. Modes TE10 and TE01 are fed by the fundamental mode TE10 of rectangular waveguides of port 1 and port 2, respectively. As shown in Fig. 3 (a) and 3 (b), the diagonal horn transitions slowly from the rectangular waveguide to the diagonal horn, when the $l_p = 5.04$ mm. As the width of diagonal structure increases, mode TE01 becomes feasible and port 2 is introduced when $l_6 = 13$ mm. Fig. 3 (c) show the current distribution when port 1 and port 2 are fed, respectively. It is observed that the

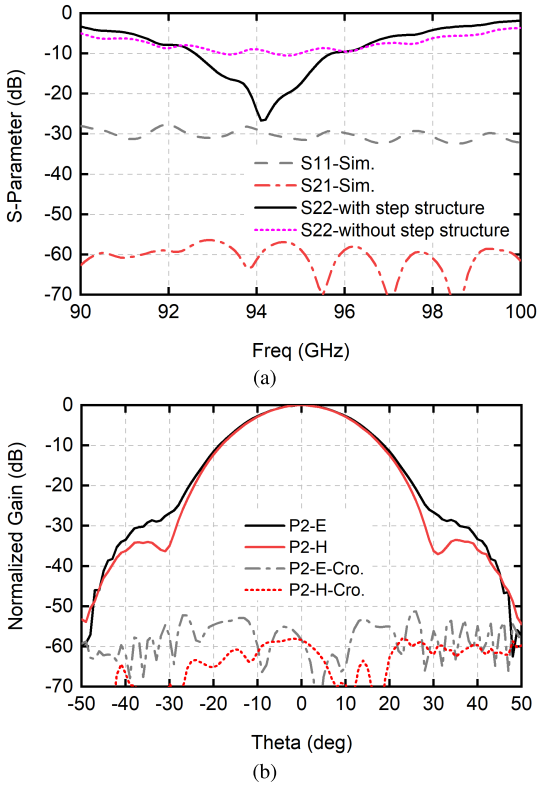

FIGURE 4. (a) Simulated S-parameters and (b) E-H plane radiation patterns of the feed system when port 2 is fed.

feeding position of port 2 is exactly at the position where the current of port 1 is low, which can improve the isolation between two ports and reduce the influence on the current distribution of port 1. In comparison with the scheme structure of conical horn, the use of a diagonal horn antenna is beneficial for obtaining higher port isolation. WR10 is used in two ports. After optimization, the final dimensions (in mm) are $a_1 = 9$, $l_1 = 77.6$, $l_2 = 30$, $l_3 = 10$, $l_4 = 10$, $l_5 = 24.365$, $l_6 = 13$, $l_7 = 4.27$, $h_1 = 0.385$, $h_2 = 0.35$, $w_1 = 1.7$, $w_2 = 1.04$, and $w_3 = 0.4$.

Fig. 4 (a) shows the simulated S-parameters of the antenna feed system: Port 1 is well matched within the range 90–100 GHz, $S22$ is less than -15 dB from -93 to 95.3 GHz, and the isolation $S21$ between the two ports is better than -58 dB. Because the two ports have almost the same simulated radiation pattern, and it is good for the consistency of two port's E-H plane radiation pattern of the designed cassegrain. So, in Fig. 4 (b), only the E-H plane's radiation pattern of port 2 is shown. As shown in Fig. 4 (b), the E-H plane's radiation pattern has a similar gain curve within an angle of 20°, and the cross polarization is better than 50 dB.

C. SIMULATION OF THE COMPLETE ANTENNA SYSTEM

To evaluate the performance of the entire antenna system, HFSS was used in the simulation. In the simulation works, copper was selected as the material for the feed horn system and sub-reflector, whereas aluminum was selected as the material for the main reflector. To save the computational

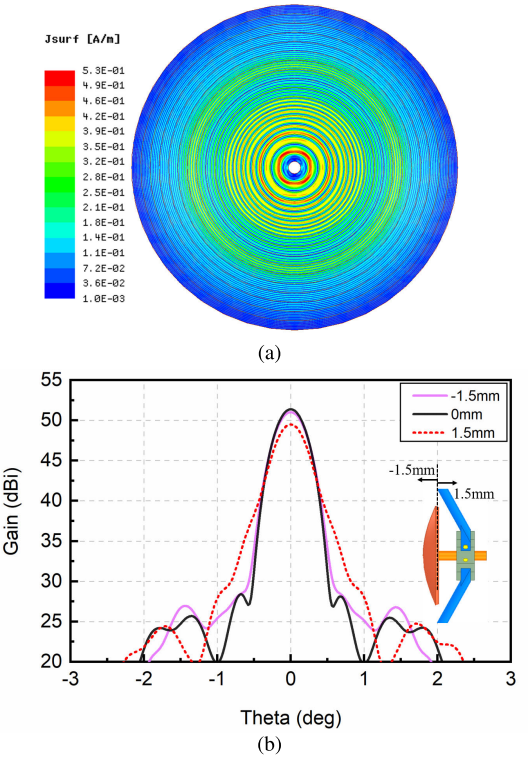

FIGURE 5. (a) Current distribution of the main-reflector and (b) efficiency of the offset of sub-reflector on the radiation pattern.

resources required for the simulation of the complete antenna, the support of the sub-reflector was not considered during the simulation. As shown in Fig. 5 (a) the current distribution of the main reflector was symmetrical, and it's useful for obtaining symmetric radiation pattern of the cassegrain antenna. This proves the design of antenna feed system based on diagonal horn antenna is reasonable and suitable.

Because the position of the sub-reflector has an important effect on the performance of the antenna, it plays an important role in the debugging and use of the antenna [21]. As shown in Fig. 5 (b), because the antenna operates at 94 GHz, even a small position offset of the sub-reflector has a significant influence on the antenna gain and side lobes. When the sub-reflector moves toward to the feed horn (−1.5mm), the side-lobe level is mainly affected, and when the sub-reflector moves far away (1.5mm), the antenna gain is mainly affected. If there is no position offset, the antenna gains are 51.45 dBi, the side lobes are −24 dB.

Due to the high operating frequency of designed antenna, the position and structure of the sub-reflector support will affect the radiation pattern of the antenna. The influence is greatest when the direction of the support structure is parallel to the E-Plane of the radiation pattern. Since the designed antenna is operated in dual-polarization, in order to take into account the performance of the antenna radiation pattern under two polarization, the support structure is selected at 45 degrees ($\varphi_1 = 45°$) with two polarization directions.

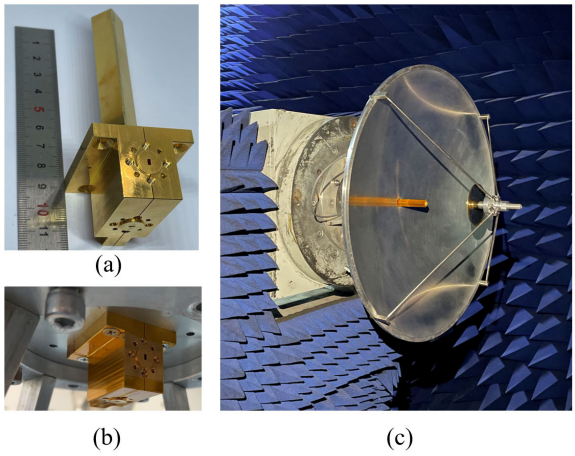

FIGURE 6. (a) Photograph of the antenna feed system and (b) assembled on deep of the main reflector. (c) Photograph of the antenna system tested in a microwave anechoic chamber.

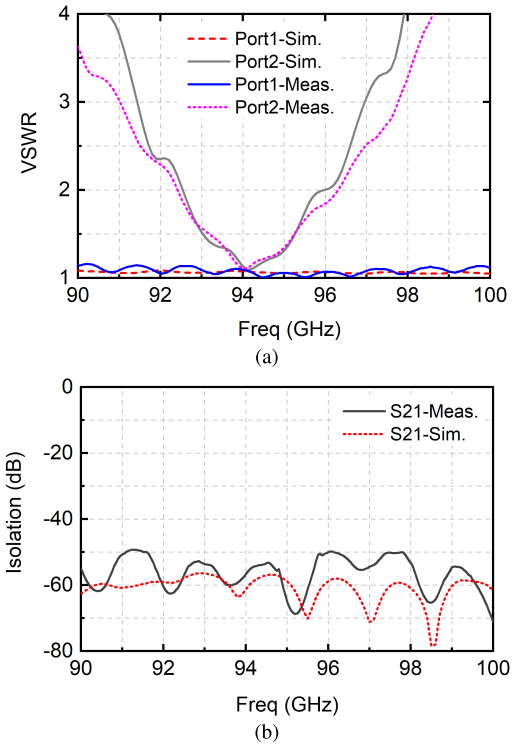

FIGURE 7. Simulated and measured results of (a) VSWR, (b) isolation and (c) radiation pattern of the feed system when port 2 is fed.

III. MEASUREMENT RESULTS

As shown in Fig. 6, An antenna was fabricated and tested. Vacuum brazing technology is used in the processing of the feed antenna and CNC for the sub and main reflectors. Vacuum brazing technology can reduce the influence of the splitting gap on the S parameter and radiation pattern of the feed system.

The radiation pattern was tested by a microwave compact field system in microwave anechoic chamber, and the

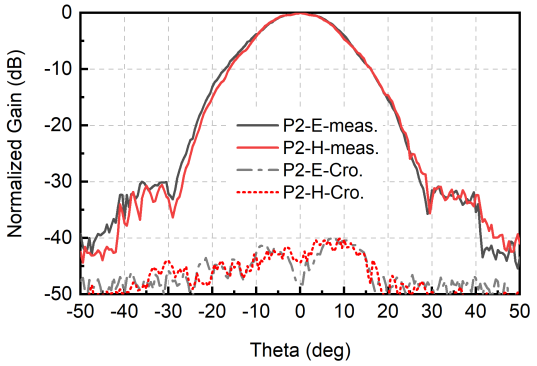

FIGURE 8. Measured results of E-H radiation patterns of the feed system when port 2 is fed.

VSWR was tested using an Agilent vector network analyzer. As shown in Fig. 7 (a), the VSWR of port 2 is less than 1.5:1 in the range 93.2–95.3 GHz, and port 1 is well matched in the entire band of 90–100 GHz. And the isolation between the two ports is greater than 50 dB in the range 93.2–95.3 GHz, as shown in Fig. 7 (b). In general, the measurement results are consistent with the simulations. Fig. 8 shows the measurement result of the E-H plane radiation patterns of port 2. Comparing with the simulation result, as shown in Fig. 4 (b), the −11 dB width is about 35°, witch 5° less than the simulation result, and the cross-polarization is above 10 dB higher than the simulation result. The difference between simulation and measurement results affects the aperture efficiency and the polarization characteristics of the designed antenna, which will be proved in the test results of the radiation pattern in Fig. 9.

Fig. 9 shows the measurement and simulation results of the E-H planes radiation patterns when two ports are fed, respectively. On the whole, as shown in Fig. 9 (a) and 9 (b), the antenna gains, fed by port 1, are 50.85 dB and 0.6 dB lower than the maximal gain in the simulation, the side lobe is −24.5 dB, and the −3 dB beam width is about 0.45°. This might be because the angle separation rate of the test system is not sufficiently high that the first side lobe of −22 dB that exists in the simulation is not shown in the test results. Benefiting from the feed method and matching of port 2, as shown in Fig. 9 (c) and 9 (d), the simulation and test results of the E-H planes of the radiation pattern and the other performances are consistent with the results of port 1. This characteristic of the two ports is very important in these applications. From Fig. 9, the tested cross polarization of the E-H plane of each port are above −40 dB and about 8 dB lower than the simulation at the direction of E-H radiations. In general, the curves of the radiation pattern shown in Fig. 9 are consistent with the simulation results. The simulated and tested results show that the aperture and radiation efficiency are above 53% and 83%, and the aperture efficiency is affected for lower side lobes. Referring to the simulated current distribution of the main reflector and the radiation pattern of feed horn, as shown in Fig. 5 (a) and Fig. 8, the current amplitude at

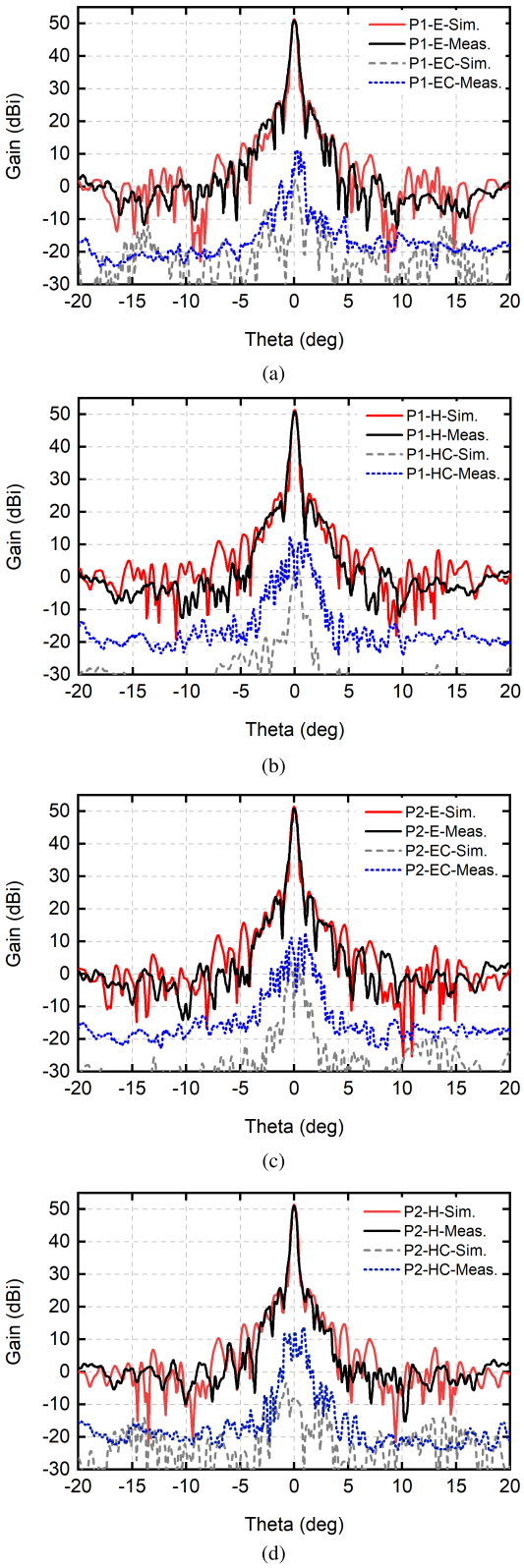

FIGURE 9. Measured and simulated results of antenna radiation pattern, and cross polarization level at 94 GHz.

the edge of the main reflector of the antenna is relatively low. The performance of cross-polarization is affected by the

TABLE 1. Performance comparisons between the designed antenna and existing W-band reflector and cassegrain antennas.

Ref.	Antenna Type	Antenna Size (mm)	3dB Band-width	Peak Gain/dB	Pol-arizaiton
[22]	off-set	150*210	N/A	41.0	single
[23]	Cassegrain	D=300	1.42^o	41.3	single
[11]	Cassegrain	D=500	0.56^o	50.1	N/A
[13]	Cassegrain	D=500	0.54^o	49.5 47.3	dual
[6]	Cassegrain	D=800	0.45^o	51.3	single
[12]	Cassegrain	D=900	0.3^o	54.5	single
[24]	off-set Cassegrain	D=300 D=1200	0.6^o 0.3^o	46.4 55.0	dual
[25]	Cassegrain	D=1200	0.18^o	59.45	dual
[14]	Cassegrain	D=1850	0.12^o	63.1	single
[26]	Cassegrain	D=2500	0.09^o	N/A	dual
This Work	Cassegrain	D=540	0.45^o	50.85	dual

radiation characteristics of the feed horn and the antenna's installation error. It is found that the cross-polarization of the antenna is easily affected by the little position change of the sub-reflector and the feed horn in the MMW-band. Table 1 gives a performance comparison among designed and existing W-band reflector and cassegrain antennas. The performance shows that the designed dual-polarization antenna is suitable for the MMW cloud radar systems.

IV. CONCLUSION

In this paper, a dual-polarization high-isolation cassegrain antenna is presented, fabricated, and tested. In the design, a diagonal horn feed antenna is fed with two ports perpendicular to each other for good polarization isolation performance. The HFSS software was used for the simulation and optimization to obtain the ideal performance of the antenna system. The test results demonstrate that the VSWRs of port 1 and 2 are well matched in the range 93.2–95.3 GHz, and the isolation between two ports is better than 50 dB in the range 93.2–95.3 GHz. The antenna gains are 50.85 dBi, the side-lobe levels are -24.5 dB, the cross polarization is above -40 dB at the direction of E-H radiations. The designed method of feed system is suitable in the design of large size and higher frequency dual-polarization antennas. Overall, the test results are consistent with the simulations, and the proposed W-band dual-polarization antenna has successfully used in designed W-band cloud radar systems.

ACKNOWLEDGMENT

The authors would like to acknowledge the MMW-Laboratory for the technical support of measurement and debug.

REFERENCES

[1] G. J. Linde, M. T. Ngo, B. G. Danly, W. J. Cheung, and V. Gregers-Hansen, "WARLOC: A high-power coherent 94 GHz radar," *IEEE Trans. Aerosp. Electron. Syst.*, vol. 44, no. 3, pp. 1102–1117, Jul. 2008.

[2] T. Takano, Y. Nakanishi, H. Abe, J. Yamaguchi, S.-I. Yokote, K.-I. Futaba, Y. Kawamura, H. Kumagai, Y. Ohno, T. Takamura, and T. Nakajima, "Performance of a developed low-power and high-sensitivity cloud profiling millimeter-wave radar: FALCON-I," in *Proc. Asia–Pacific Microw. Conf.*, Dec. 2007, pp. 1–4.

[3] R. R. Neely, III, L. Bennett, A. Blyth, C. Collier, D. Dufton, J. Groves, D. Walker, C. Walden, J. Bradford, B. Brooks, F. I. Addison, J. Nicol, and B. Pickering, "The NCAS mobile dual-polarisation Doppler X-band weather radar (NXPol)," *Atmos. Meas. Techn.*, vol. 11, no. 12, pp. 6481–6494, Dec. 2018.

[4] Y. Wang and V. Chandrasekar, "Polarization isolation requirements for linear dual-polarization weather radar in simultaneous transmission mode of operation," *IEEE Trans. Geosci. Remote Sens.*, vol. 44, no. 8, pp. 2019–2028, Aug. 2006.

[5] C. Granet, J. S. Kot, T. Natusch, S. Weston, and S. Gulyaev, "Design of an X-band feed system for the Auckland university of technology 30 m diameter warkworth radio telescope," in *Proc. 11th Eur. Conf. Antennas Propag. (EUCAP)*, Mar. 2017, pp. 3621–3625.

[6] J. Wang, J. X. Ge, Y. Zhou, H. Xia, and X. Z. Yang, "Design of a high-isolation 35/94-GHz dual-frequency orthogonal-polarization Cassegrain antenna," *IEEE Antennas Wireless Propag. Lett.*, vol. 16, pp. 1297–1300, 2017.

[7] S. Adibelli, P. Juyal, C.-L. Cheng, and A. Zajic, "Terahertz near-field focusing using a 3-D printed Cassegrain configuration for backscattered side-channel detection," *IEEE Trans. Antennas Propag.*, vol. 67, no. 10, pp. 6627–6638, Oct. 2019.

[8] A. Passarelli, C. Koral, M. R. Masullo, W. Vollenberg, L. L. Amador, and A. Andreone, "Sub-THz waveguide spectroscopy of coating materials for particle accelerators," *Condens. Matter*, vol. 5, no. 1, p. 9, Jan. 2020.

[9] H. J. Gibson, B. Thomas, L. Rolo, M. C. Wiedner, A. E. Maestrini, and P. de Maagt, "A novel spline-profile diagonal horn suitable for integration into THz split-block components," *IEEE Trans. THz Sci. Technol.*, vol. 7, no. 6, pp. 657–663, Nov. 2017.

[10] D. A. Montofre, R. Molina, A. Khudchenko, R. Hesper, A. M. Baryshev, N. Reyes, and F. P. Mena, "High-performance smooth-walled horn antennas for THz frequency range: Design and evaluation," *IEEE Trans. THz Sci. Technol.*, vol. 9, no. 6, pp. 587–597, Nov. 2019.

[11] A. Myagkov, S. Kneifel, and T. Rose, "Evaluation of the reflectivity calibration of W-band radars based on observations in rain," *Atmos. Meas. Techn.*, vol. 13, no. 11, pp. 5799–5825, Nov. 2020.

[12] P. Kollias, N. Bharadwaj, K. Widener, I. Jo, and K. Johnson, "Scanning ARM cloud radars. Part I: Operational sampling strategies," *J. Atmos. Ocean. Technol.*, vol. 31, no. 3, pp. 569–582, Mar. 2014.

[13] B. Yu, H. Xia, X. Chen, F. Yang, and J. X. Ge, "A novel W-band dual-polarized Cassegrain antenna for cloud radar," *Prog. Electromagn. Res. Lett.*, vol. 61, pp. 99–103, 2016.

[14] S. Spitz, A. Prata, J. Harrell, R. Perez, and W. Veruttipong, "A 94 GHz spaceborne cloud profiling radar antenna system," in *Proc. IEEE Aerosp. Conf.*, Mar. 2001, pp. 2/685–2/694.

[15] W. L. Stutzman and G. A. Thiele, *Antenna Theory and Design*. Hoboken, NJ, USA: Wiley, 2012.

[16] C. A. Balanis, *Antenna Theory: Analysis and Design*. Hoboken, NJ, USA: Wiley, 2015.

[17] A. Gonzalez and S. Asayama, "Double-ridged waveguide orthomode transducer (OMT) for the 67–116-GHz band," *J. Infr., Millim., THz Waves*, vol. 39, no. 8, pp. 723–737, Aug. 2018.

[18] H. Saeidi-Manesh, S. Saeedi, M. Mirmozafari, G. Zhang, and H. H. Sigmarsson, "Design and fabrication of orthogonal-mode transducer using 3-D printing technology," *IEEE Antennas Wireless Propag. Lett.*, vol. 17, no. 11, pp. 2013–2016, Nov. 2018.

[19] C. A. Leal-Sevillano, Y. Tian, M. J. Lancaster, J. A. Ruiz-Cruz, J. R. Montejo-Garai, and J. M. Rebollar, "A micromachined dual-band orthomode transducer," *IEEE Trans. Microw. Theory Techn.*, vol. 62, no. 1, pp. 55–63, Jan. 2014.

[20] K. B. Kong, H. S. Kim, R. S. Aziz, and S. O. Park, "Design of offset dual-reflector antennas for improving isolation level between transmitter and receiver antennas," *Prog. Electromagn. Res. C*, vol. 57, pp. 193–203, 2015.
[21] A. Demirci, N. Sonmez, F. Tokan, and N. T. Tokan, "Phase error analysis of displaced-axis dual reflector antenna for satellite earth stations," *AEU-Int. J. Electron. Commun.*, vol. 110, Oct. 2019, Art. no. 152824.
[22] K. B. Cooper, R. R. Monje, R. J. Dengler, C. J. Cochrane, M. Alonso-Delpino, A. Tang, T. O. El Bouayadi, and O. Pradhan, "A compact, low power consumption, and highly sensitive 95 GHz Doppler radar," *IEEE Sensors J.*, vol. 20, no. 11, pp. 5865–5875, Jun. 2020.
[23] E. Nova, D. Rodrigo, J. Romeu, and L. Jofre, "94 GHz Cassegrain reflector antenna performance characterization," in *Proc. 6th Eur. Conf. Antennas Propag. (EUCAP)*, Mar. 2012, pp. 3442s3445.
[24] L. Li, G. M. Heymsfield, P. E. Racette, L. Tian, and E. Zenker, "A 94-GHz cloud radar system on a NASA high-altitude ER-2 aircraft," *J. Atmos. Ocean. Technol.*, vol. 21, no. 9, pp. 1378–1388, 2004.
[25] P. M. Koch *et al.*, "1.2 M shielded Cassegrain antenna for close-packed radio interferometer," Dec. 2010, *arXiv:1012.3899*.
[26] A. J. Illingworth *et al.*, "The EarthCARE satellite: The next step forward in global measurements of clouds, aerosols, precipitation, and radiation," *Bull. Amer. Meteorol. Soc.*, vol. 96, no. 8, pp. 1311–1332, Aug. 2015.

JIE WANG (Graduate Student Member, IEEE) received the B.S. degree in network communication from Henan University, Henan, China, in 2013, and the M.S. degree in electrical engineering (telecommunication) from the Nanjing University of Information Science and Technology, Nanjing, China, in 2017, where he is currently pursuing the Ph.D. degree. His current research interests include electromagnetic scattering theory, microwave and millimeter-wave antenna, and frequency-selective surface (FSS).

HAI LIN (Graduate Student Member, IEEE) received the B.S. degree in electrical electronic and information engineering from the Nanjing University of Information Science and Technology, Nanjing, China, in 2016, where he is currently pursuing the Ph.D. degree. His current research interests include electromagnetic scattering theory and radar signal processing.

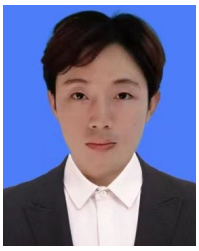

FAN YANG received the B.E. degree from Shaoyang University, Shaoyang, China, in 2018. He is currently pursuing the M.S.E. degree in information and communication engineering with the Nanjing University of Information Science and Technology, Nanjing, China. His research interests include radar signal processing and adaptive beamforming algorithm.

GUANGYANG XU (Student Member, IEEE) was born in Suqian, China. He received the B.E. degree in communication engineering from the Henan University of Engineering, Zhengzhou, China, in 2019. He is currently pursuing the master's degree in information and communication engineering with the Nanjing University of Information Science and Technology, Nanjing, China. His current research interests include microwave devices and array antennas.

JUNXIANG GE (Member, IEEE) received the Ph.D. degree in radio engineering from Southeast University, Nanjing, China, in 1991. From February 1982 to July 1986, he was a Research Assistant at NUAA. He was a Postdoctoral Fellow at the University of Electronic Science and Technology (UESTC), Chengdu, China, from December 1991 to October 1993. In October 1993, he joined the Beijing University of Aeronautics and Astronautics (BUAA), Beijing, China. From November 1992 to October 1994, he was an Assistant Professor of UESTC and BUAA. In November 1994, he became a Professor of BUAA. From August 1995 to March 1998, he was the Head of the Department of Electronic Engineering, BUAA. From November 1997 to February 1998, he was a Visiting Professor to research W-CDMA mobile communication systems at NTT DoCoMo, Yokosuka, Japan. From April 1998 to March 1999, he was a Center of Excellence (COE) Research Fellow to research millimeter waves and optical technology at the Communication Research Laboratory, Ministry of Telecommunications of Japan, Tokyo, Japan. From April 1999 to January 2011, he joined YoKoWo Company Ltd., Tokyo, as the Deputy General Manager of the Research and Development Department. In January 2011, he joined the Nanjing University of Information Science and Technology, Nanjing, China, as the Dean of the Department of Electronic Engineering, where he has been the Dean of the School of Electronic and Information Engineering, Nanjing, since 2011. He has authored or coauthored over 60 articles and over ten patents. His current research interests include electromagnetic field theory and microwave and millimeter-wave technology and antennas.